Radiative transitions associated with hole confinement at Si δ-doped planes in GaAs

Mao-Long Ke, J. S. Rimmer, and B. Hamilton
Department of Pure and Applied Physics, The University of Manchester, Institute of Science and Technology, Manchester M60 IQD, United Kingdom

J. H. Evans, M. Missous, and K. E. Singer
Department of Electrical Engineering and Electronics, The University of Manchester, Institute of Science and Technology, Manchester M60 IQD, United Kingdom

P. Zalm
Philips Research Laboratories, P.O. Box 80000, 56000JA, Eindhoven, The Netherlands
(Received 2 July 1991; revised manuscript received 6 January 1992)

Spatially direct radiative processes involving δ-doped planes are reported. The transitions are observed in structures that were designed to strongly confine holes to the δ planes. Two structures, δ-plane superlattices and center-δ-doped quantum wells were used. In each case low-dimensional features associated with the modified subband structure were observed. The δ-plane superlattices exhibit electron minibands that may be "tuned" by control of the δ-plane spacing. Photogenerated holes are trapped in such structures and are unable to transport in the growth direction at low temperatures. The δ-doped quantum wells show grossly shifted confined states; for the heaviest doped well measured, the normal ordering of the $n=1$ light-hole and the $n=2$ heavy-hole states is reversed. Self-consistent calculations are reported, which account for the optical data in both types of structure.

I. INTRODUCTION

Low-dimensional semiconductor systems exhibit strong excitonic effects as a result of the confinement and correlation properties of electronic particles. The luminescence and absorption spectra of quantum-well structures are often dominated by excitonic transitions; indeed, much of our understanding of the electronic structure of such systems derives from the analysis of the optical properties of excitons.[1,2]

The advances in epitaxial growth, which have fueled the science of heterojunction systems, have also led to the ability to place dopant spikes with great precision. In such δ- (or atomic plane) doped layers, the core charge of the impurity atoms is partially screened by those electrons (we consider only donor impurity planes in this paper) which remain localized to the dopant plane. The net result is a self-consistent δ potential which forms a cusp-like quantum well in the conduction band. The detailed shape of the well must be obtained by self-consistently solving the Schrödinger and Poisson equations. This is a fundamental requirement because the screening properties of the electrons in each subband differ greatly according to the form of the wave function normal to the δ plane.[3–5]

δ doping is of great importance for device applications, especially for field-effect-transistor structures,[6] which are increasingly used for fast logic. These structures generally utilize a single δ plane, and exploit transport properties of the conduction-band quantum well formed by the dopant sheet. The confined states in the conduction-band well have also been shown to exhibit strong resonant absorption in the infrared. Moreover, this absorption can be tuned because the depth and shape of the well is a function of the two-dimensional gas density.[7] There is to date, however, little published data on band-gap-related optical transitions involving isotype (single impurity) δ planes. This is not surprising since the valence-band bending near the δ plane mirrors the conduction band, and in the case of a donor plane is repulsive to a photogenerated hole: the δ plane induces a type-II quantum well. Radiative recombination that involves electrons localized in the plane is therefore spatially indirect and intrinsically weak. The ability to localize the hole to the δ plane would be expected to change radically the optical transitions. This can be achieved, in principle, by modifying the environment of the δ plane; for example, an electrostatic barrier formed by an adjacent doping structure or a nearby heterojunction barrier would both serve to confine a photoinjected hole. Recent attempts to do this[8–10] have proved successful, and open up the possibility of exploiting photoluminescence as a probe for analyzing δ-doped structures.

In this paper we describe experiments which demonstrate such hole confinement at very short ranges, essentially in the quantum limit. Two structures are evaluated, short-period isotype δ-plane superlattices and center-δ-plane-doped quantum wells. In each case electronic features are observed which represent a modification of the (isolated) δ-plane properties, and which result from the quantum scale of the confinement. In the case of the δ-plane superlattice we observe clear electron miniband formation. In the center-doped quantum-well structures, we demonstrate that the hetero-

junction confinement radically changes the electron screening behavior. The depth of the δ potential, compared to that of an isolated plane in bulk material, and the subband structure for both electrons and holes (compared to those of an undoped well) are self-consistently modified to an extent which is dependent on the electron density. The experimental data are supported by self-consistent calculations of subband structure within the effective-mass approximation. In the next section we review the general features of the structures used in this work; in Sec. III photoluminescence (PL) and photoluminescence excitation spectroscopy (PLE) data obtained from the superlattice are presented and analyzed, and in Sec. IV, quantum-well PL and PLE data are presented and analyzed. Both structures have been analyzed with reference to the calculated structures.

II. QUANTUM-SCALE HOLE-CONFINING STRUCTURES

The optical activity of the δ layers, induced by hole confinement, is shown schematically for both types of structure in Fig. 1. The diagrams have been appropriately scaled in order to illustrate two of the measured structures. As the hole confinement approaches the quantum limit, electron minibands are formed in the case of the superlattice [Fig. 1(a)]. For the δ-doped quantum well the hole potential includes a central barrier that significantly perturbs the confined states and which for heavily δ-doped wells evolves into two coupled wells, as illustrated in Fig. 1(b).

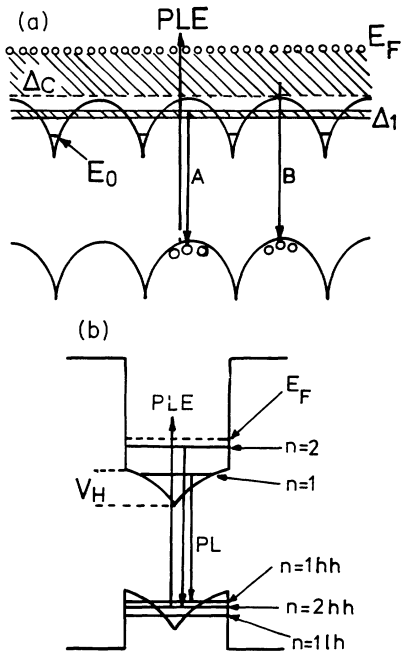

FIG. 1. Schematic illustrations of the hole-confinement structures used in this work. The transitions measured are also illustrated. (a) illustrates the potential variation for a δ-plane superlattice. The detailed potential depends critically on the δ-plane spacing, but may lead to miniband formation for the low-effective-mass electrons. Hole miniband formation does not occur. Trapping of photogenerated holes between the δ planes leads to strong optical activity. (b) shows the potential associated with a center-δ-doped quantum well. The figure is scaled to illustrate a 120-Å well doped with a 5×10^{12} cm^{-2} Si sheet. The states are labeled with energy quantum number n, and the heavy (hh) and light hole (lh) states are distinguished.

We consider first the short-period δ-plane superlattices. When a short-period isotype δ superlattice of the correct geometry is grown, two important conditions may be met which increase the efficiency of band-gap-related optical transitions. First, electron states may couple to form minibands (we shall refer to these as Δ bands) with associated extended electron wave functions. Second, optically injected holes may be trapped *between* adjacent (repulsive) δ planes and so are available for recombination. The strength of the radiative recombination will clearly depend on the electron and hole wave-function overlap in the region between the dopant planes. The large effective mass of the hole does not favor miniband formation, and we expect inter-dopant-plane confinement to dominate in the structures described here.

A δ-plane superlattice can be formed by growing epitaxial material such as GaAs by molecular-beam epitaxy (MBE) that contains closely spaced sheets of dopant atoms (e.g., Si). Such a superlattice is distinct from, for example, a $n-i-p-i$ structure in that the δ system may be completely n type, and the periodic potential is described by the array of interacting self-consistent δ potentials. The interaction strength is crucial because it controls the shape of the periodic potential which can only be calculated by self-consistent methods. The subband structure of $n-i-p-i$ and δ-plane $n-i-p-i$ superlattices has been calculated on the assumption that the potential distribution originates from unscreened impurity charges.[11,12] That is, the periodic potential in thermal equilibrium is that of a fully compensated structure and is fixed in the same sense as that of an undoped heterostructure system; such systems do not require self-consistent solutions.

Optical techniques which probe the subband structure have not been widely applied to δ superlattices. PL and Raman-scattering measurements of periodically δ-doped Si:GaAs have been reported[13] in which the sheet separation was varied between 10 and 50 nm. The Raman-scattering results suggest that conduction minibands are present when the δ planes are sufficiently close to each other.

The spatial localization of the impurity atoms which form the doping sheets is influenced by thermally induced diffusion during subsequent growth.[14,15] However, it is clear that, provided a large enough density of dopant has been selected so that a degenerate system can be formed, δ doping sheets do form two-dimensional electron gas systems.[16] It has emerged from our work that the actual dopant spread (within a few nm) is at least an order of magnitude less than the intersheet distance required for clear optical activity from the superlattice, and as such does not significantly affect the miniband energies.

The center-δ-doped quantum wells investigated in this work perform the same confinement task for the hole as demonstrated in the work of Wagner and coworkers,[8-10] enhancing photoluminescence compared to

that of an isolated δ sheet.[17] However the confinement in the present case is in the quantum limit and results from both heterointerface band offsets and the doping-plane potential. The δ-plane potential is itself modified by the presence of the heterojunctions which results in a self-consistent subband structure. This represents a new class of combined heterojunction-δ (HD) low-dimensional system. The perturbation to the undoped case can be severe both for the electron and the hole states. We argue below that for the hole with its high effective mass and small confinement-energy shift, the δ doping can effectively induce a double quantum well in the valence band. Significant changes in optical properties may result. Again, the subband structure must be solved self-consistently, and the self-consistent component of the quantum-well potential is dissimilar from that of an isolated δ potential because the heterojunction barriers modify the screening problem. In this type of hole-confining structure, transitions involving the electrons associated with the δ plane may now be truly direct in real space, since the hole states and associated wave functions spread across the entire width of the quantum well.

A center-δ-doped quantum well is an alternative way to introduce a high carrier density into the well. In general, the stability of excitons is reduced at high carrier densities (by virtue of either doping or excitation), because the Coulomb interaction becomes progressively screened as the electron or hole density increases. However, in heavily doped systems, an excitonlike resonance may still exist due to electron-hole scattering processes which occur on the Fermi sea. Such many-body interactions, which result in a Fermi-edge singularity (FES) or Mahan exciton, have been reported by several groups for the case of modulation-doped quantum wells.[18–21] We have examined the influence of the δ doping level on the resonancelike absorption behavior of the quantum wells.

In this paper, we report PL and PLE measurements on ten-period δ-doped superlattices. The evolution of the superlattice miniband structure as the period reduces is clearly seen in the PL data and confirmed by the PLE measurements. We also report PL and PLE measurements on a limiting case of an HD structure consisting of a 120-Å-wide GaAs quantum well, center-doped with a single silicon δ sheet. Three values of sheet-doping density were measured. In these structures, hole confinement in the quantum well clearly plays an important role. The emission is strong, which is a consequence of the spatially direct nature of the transitions. The detailed PL and PLE spectra reflect the subband structure of the HD system. We briefly present the results of self-consistent calculations for both types of structure which support the spectroscopic trends observed.

III. δ-DOPED SUPERLATTICES

The δ superlattices, each containing ten δ planes, were grown in an all-solid-source VG90 MBE system. Three structures were grown, with 100- 350-, and 1000-Å periods, respectively. The Si atomic concentration was adjusted to yield 5×10^{12} cm^{-2}; at this doping level the sheet electron density is expected to be the same as the sheet atomic density. The growth conditions were adjusted so that the samples were grown under minimal As_4 to Ga flux ratio; to reduce dopant migration, a growth temperature of ~520 °C was chosen.[22] A 1-μm undoped buffer layer was grown before deposition of the superlattice. Precise control of the periodicity of the superlattice was achieved by computer control of the Ga, Si, and As shutters, which ensured reproducible growth conditions.

Secondary-ion-mass-spectroscopy (SIMS) measurements were carried out on the δ superlattice structures in order to confirm the δ-plane separation, and also to gauge the dopant spread during the total growth period. A CAMECA IMS 4F system was used for this work, which employed a rastered O_2^+ primary beam at an ion current of 150 nA. Positive secondary ions from the center of the crater and with energies in excess of 25 eV were analyzed. After calibrating the system by comparison with a 50-keV implanted Si:GaAs layer, we were able to confirm the precise periodicity and impurity localization of the superlattices. Figure 2 illustrates the SIMS profile of the δ superlattice with sheet spacing 350 Å. The symmetrical shape of the individual spikes indicates that the observed broadening is due to thermal diffusion occurring during subsequent growth.

The electronic structure of a single δ sheet has been calculated previously,[6,11] but not that of a δ superlattice. We have modeled the superlattice energy-band structure using a self-consistent Hartree calculation. This takes account of the electron population in all subbands, including the Δ bands, and also in the continuum which exists fractionally above the Hartree potential. A summary of our model is presented here; a detailed description will be presented elsewhere. The Schrödinger equation within the effective-mass approximation is solved self-consistently with the Poisson equation. The calculation assumes that the superlattice conduction- (and valence-) band-edge energy variation in the growth direction is determined by the periodic screened potential due to the planes of ionized donors. The occupancy of all states, both localized (in the growth direction) and extended, was taken into account.

Figure 3(a) shows the general trend in the shape of the

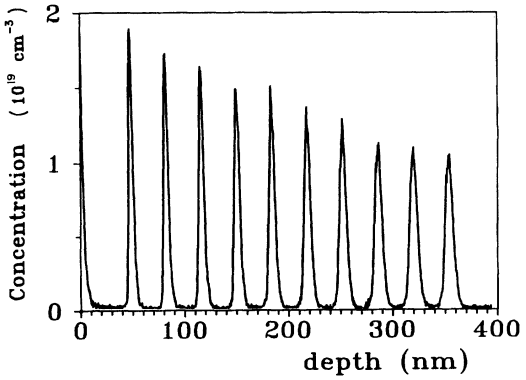

FIG. 2. SIMS profile of a ten-period δ superlattice with sheet spacing of 350 Å. The symmetrical shape of the individual spikes indicates that the broadening is due to thermal diffusion occurring during subsequent growth.

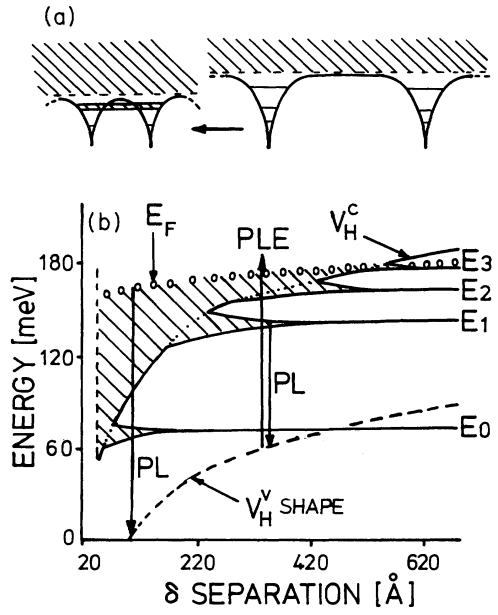

FIG. 3. (a) illustrates the change gross features of a δ superlattice as the spacing between δ planes is decreased. The depth of the Hartree potential is reduced, bands broaden, and higher bands merge into the continuum. The calculated electronic structure as a function of sheet separation is shown in (b). The Δ bands are labeled in accordance with the text. Cross hatching indicates filled bands.

superlattice potential and miniband evolution as the δ-plane separation is reduced. The major effect of decreasing the separation is to lower the self-consistent Hartree potential V_H, and to broaden the discrete states of the isolated δ planes into minibands as the interaction energy increases. The evolution of the electronic structure of the δ superlattice as the δ-plane spacing is varied, calculated for a sheet dopant density of 5×10^{12} cm^{-2}, is shown in Fig. 3(b). The top of the Hartree potential in the valence band V_H^v has been arbitrarily shifted and is included purely to illustrate transitions. The ground state for optical transitions is at V_H^v, midway between adjacent δ planes, where photoinjected holes rapidly collect. Since $V_H^v = V_H^c - E_g$, where V_H^c is the top of the Hartree potential in the conduction band, the calculation predicts that transitions may occur at energies both above and below E_g, and the data confirm this.

When the δ-sheet spacing is large, lower confined states are uncoupled and retain the character of isolated δ planes, i.e., electrons are confined in the growth direction but occupy extended two-dimensional subbands in the dopant sheet plane. For all separations there exists a continuum band Δ_c fractionally above the Hartree potential which is largely unoccupied for separations greater than 700 Å. As the intersheet spacing decreases, the states E_3, E_2, E_1, and E_0 begin to couple. The coupling between the lowest (E_0) states is not strong, with a Δ-band width of less than 10 meV at a sheet separation of 100 Å. Also, as the separation decreases, an increased number of electrons appear in Δ_c above the Hartree potential, because the Fermi level has moved up in energy relative to the hole ground-state energy. At intersheet distances of <100 Å the conduction-band structure consists of Δ bands only, with no localized states.

The density of states [$\mathbf{D}(E)$] in Δ_c is assumed in the model to be three dimensional, and therefore only the bottom of this band is indicated in Fig. 3(b). A two-dimensional $\mathbf{D}(E)$ is used for the confined states. At the onset of the coupling of states, $\mathbf{D}(E)$ for the narrow Δ bands can be described by a ten-level closely spaced two-dimensional model. When the lower Δ bands rise in energy and interact with Δ_c, $\mathbf{D}(E)$ is totally dominated by the three-dimensional model, and this is illustrated in Fig. 3(b) by the narrow Δ bands "merging" with Δ_c.

Photoluminescence (PL) measurements were carried out with the 514-nm line of an argon-ion laser as the excitation source, operating in a low-excitation regime where the perturbation to the majority carrier population was negligible. Detection was with a cooled GaAs photomultiplier tube, using conventional lock-in techniques. Photoluminescence excitation spectroscopy (PLE) measurements at 4 K, were made using an argon-ion pumped Ti-sapphire laser as the tunable excitation source.

Figure 4 shows PL spectra from the three superlattices. The spectra are quite different for each δ spacing, and can be explained in terms of the coupling of the δ states. Referring to Fig. 1(a), it is clear that radiative transitions occur between the Δ bands and the confined photocreated holes; these transitions are now *direct* in real space. The holes in this superlattice are confined in wells which are displaced half a superlattice period from the confined electrons that occupy uncoupled states. Therefore, the probability of radiative transitions between holes and electrons in these uncoupled states ("type-II" transition)

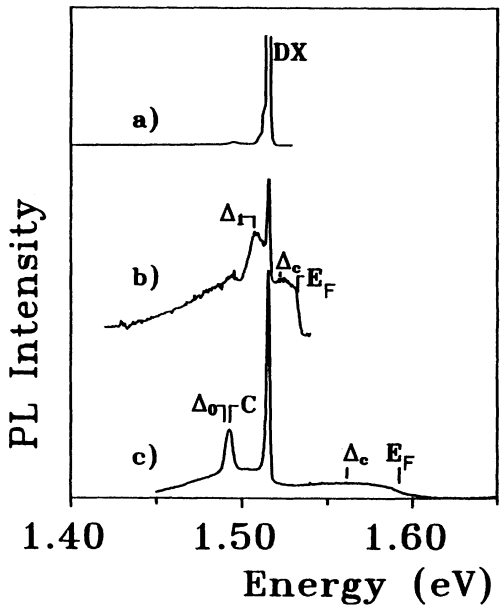

FIG. 4. Photoluminescence spectra for δ-doped superlattices with periods 1000, 350, and 100 Å, labeled in accordance with the text and in Fig. 3(b), e.g., Δ_1 refers to a full miniband, and Δ_c refers to the partially occupied band above the Hartree potential. The experimentally deduced Fermi energy relative to the hole ground-state energy is also indicated.

is much smaller than the probability of a type-I transition which involves the Δ bands. For this reason, we believe that it is the superlattice Δ bands that are involved in radiative transitions associated with δ-doped superlattices.

In the 1000-Å case, the δ sheets behave as isolated dopant planes, which are inherently optically inactive, and we observe a donor–bound exciton peak along with a weak carbon free-to-bound (FB) transition. However, as the intersheet distance is reduced, the periodic potential is modified, and the structure acquires a superlattice nature; this leads to the formation of Δ bands. These Δ bands can be clearly observed in the spectrum for the 350-Å δ spacing as features on either side of the donor–bound exciton line. Again, there is also a weak carbon FB transition. The peaks labeled Δ_1 and Δ_c are attributed to the first Δ band of the superlattice and the continuum band above the Hartree potential, respectively, rather than the uncoupled quantum-well-like states. This is in good agreement with our model: from Fig. 3(b) it can be predicted that the electronic structure of a δ superlattice with a sheet spacing of 350 Å consists of one uncoupled state at the bottom of the quantum wells, one completely fully Δ band, and the partially occupied Δ_c above the Hartree potential.

The PL spectrum from the 100-Å-period superlattice also revealed a bound exciton peak, and a high-energy plateau with a Fermi edge at 1.590 eV. We may deduce from the high-energy plateau that the Fermi level is raised with respect to the ground-state hole energy. We also observe a peak at 1.493 meV, downshifted by 1 meV with respect to the C FB transition expected from bulk GaAs, and linewidth ~5 meV. Our calculations predict that for this period, the miniband Δ_0 [see Fig. 3(b)] would yield transitions at this energy, broadened to a comparable extent. It is therefore possible that this peak contains contributions from Δ_0, convoluted with the carbon FB transitions. This is in agreement with our model, which predicts that at intersheet distances of < 100 Å there will be only Δ bands and no uncoupled states. The model also predicts that the Fermi level will have increased in energy, and this is confirmed by our observation of the Fermi cutoff at higher energies in narrower superlattices.

Another feature of the 350- and 100-Å-period samples is a broad luminescence tail which extends to lower energies. The origin of this signal is unclear but may be associated with acceptor-related transitions occurring within the superlattice (SL) structure. The valence-band edge, and therefore the acceptor-state energy, varies relative to the Δ-band energy depending on the spatial location within the SL. Transitions occurring at different points in real space will therefore have different energies, leading to a highly broadened PL spectrum.

Photoluminescence from the Δ_c band for 350-Å δ spacing exhibited a Fermi-edge shape with the half-occupancy point at 1.535 eV at 4 K. This feature, in broadened form, was still observable in PL at 40 K, by which temperature the bound exciton line was dramatically reduced due to thermalization. In order to confirm the assignment of the Fermi edge, PLE measurements were made on the layer with the 350-Å-period superlattice. Figure 5 shows the spectrum observed with the detection window

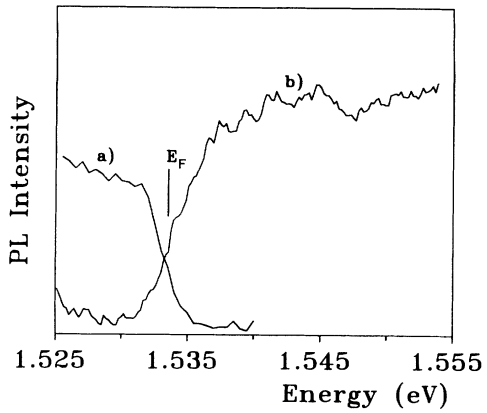

FIG. 5. The Fermi cutoff in the photoluminescence (a), and the corresponding absorption edge (b) determined by photoluminescence excitation spectroscopy for the 350-Å-period δ-doped superlattice. E_F marks the experimental deduced Fermi energy relative to the ground-state energy.

set to the peak energy of Δ_1, and compares this with the PL data. It can be seen that the absorption strength (PLE) increases as the Fermi tail of the PL drops, which is consistent with the increasing availability of final states for the absorption process. The PLE spectral form is therefore consistent with $D(E)[1-F(E)]$, where $D(E)$ is the slowly varying three-dimensional density of states, and $F(E)$ is the Fermi function of the electron gas. This form of absorption process is consistent with band-to-band processes, without excitonlike resonances. The strong overlap of the PL Fermi tail and the rising edge of the absorption edge demonstrate that negligible Stokes shift occurred in this sample.

IV. Si δ-DOPED SINGLE QUANTUM WELLS

The samples used were also grown by MBE, in a VG V90 system. After growth of a 1-μm undoped buffer layer on an n^+-type substrate, the 120-Å GaAs well was grown between 200-Å $Al_{0.3}Ga_{0.7}As$ barriers. The structures were terminated with a 300-Å capping layer. We discuss here three concentrations of δ sheet doping, corresponding to sheet electron densities of 2×10^{11}, 2×10^{12}, and 5×10^{12} cm^{-2}. In order to help reduce impurity spread, the well and δ sheet were grown at 550 °C,[23] which is lower than the conventional growth temperature for GaAs. Calculations of subband structure that include a degree of δ broadening comparable to that discussed in Sec. III indicate no significant changes when compared to the features discussed below in the context of idealized δ planes.

The confined states for both the conduction- and valence-band wells were calculated by self-consistently solving the Schrödinger and Poisson equations, in the one-particle effective-mass approximation. The calculated confined state energies, as a function of δ plane concentration, and for a fixed well width of 120 Å are shown in Fig. 6. The energies are plotted relative to the (unperturbed) three-dimensional band edge, which is the conventional reference point for confinement shifts; the calculated Fermi energy is also shown. Such calculations have been carried out previously only for a single δ

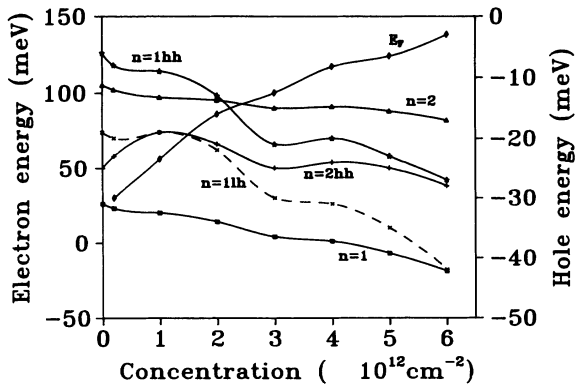

FIG. 6. Calculated electron and hole confined states as a function of δ sheet density, for a center-doped GaAs/$Al_{0.3}Ga_{0.7}$As quantum well of width 120 Å. The energies are relative to the usual reference point of the GaAs 3D band edges. The variation of the Fermi energy is also shown. The energies were calculated for the points shown, and the smooth curves are a guide to the eye.

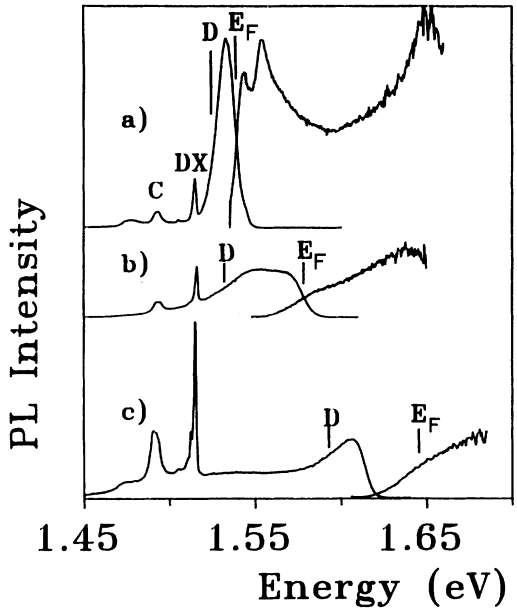

FIG. 7. Photoluminescence and PLE spectra for the center-δ-doped quantum wells with Si sheet density (a) 2×10^{11} cm^{-2}, (b) 2×10^{12} cm^{-2}, and (c) 5×10^{12} cm^{-2}. D indicates the detection energy used for the PLE measurements, and E_F the experimentally deduced Fermi energy relative to the hole ground-state energy.

sheet[24] in otherwise three-dimensional material. A temperature of 5 K was assumed in the calculation. The movement of the confined states is much more complex than the familiar picture of (for example) the variation of energy levels with quantum-well thickness. The details of this calculation will be reported elsewhere. Figure 1(b) has been scaled to illustrate the potential variation and confined states for a center-doped well with a sheet density of 5×10^{12} cm^{-2}, i.e., the heaviest doped sample measured. In this sample the $n=2$ electron subband becomes partially occupied. The depth of the Hartree cusp in all three wells is significantly reduced compared to that calculated for the equivalent isolated δ planes.[24] This is a direct consequence of the increased screening that results from the confinement of the electron wave functions by the $Al_xGa_{1-x}As$ barriers.

The influence of the δ plane on the confined states is large. For example, in the heaviest doped well, the $n=1$ electron-state energy falls to 10 meV below the conduction-band offsets. The valence-band quantum-well subbands were calculated using the self-consistent δ potential shape calculated for the conduction-band edge. Again, it emerges that significant changes in the energies of the confined hole states occurs due to the distortion of the valence-band well. One dramatic change for δ doping above approximately 2×10^{12} cm^{-2} is the reversal of ordering between the $n=1$ light-hole state and the $n=2$ heavy-hole state, compared to the familiar ordering in an unperturbed quantum well. These changes in the hole confinement energies have an important effect on the optical spectra, which are discussed below.

PL and PLE spectra are shown in Fig. 7; the PLE detection energies used are indicated in the figure. The least heavily doped structure, (a), shows a strong broad PL feature above the three-dimensional band-edge energy: the bound exciton signal from the substrate is clear, but is small compared with the up-shifted PL band. There is no clear Fermi cutoff apparent in the line shape, and the spectrum, with a half width of 10 meV, is clearly broadened compared to the spectrum of an ideal 120-Å-wide well.[25] For this structure, our calculations predict that the energy separation of the $n=1$ electron and heavy-hole subbands is 1.55 eV. We should expect the observed PL emission band to include a reduction in energy due to band-gap renormalization. In an ideal (undoped) quantum well we would also expect the transition energy to be further reduced by the exciton binding energy. However, according to our calculations for the position of the Fermi level ($E_F-E_1=7$ meV), the band-edge exciton in this structure may be destabilized. The two-dimensional (2D) renormalization energy has been calculated to be approximately 12 meV (Ref. 26) and our observed PL emission peak is at 1.533 eV. This leaves a discrepancy of 5 meV, which supports the view that the luminescence originates from a screened exciton transition and not a Fermi-edge singularity. This conclusion is in agreement with previous work[27] which demonstrates that strong band-edge-exciton effects persist in modulation-doped GaAs quantum wells with sheet electron densities less than 6×10^{11} cm^{-2}. The conclusion is further strengthened by the PLE spectrum for this sample, which shows clear heavy-hole–light-hole splitting, and which persists strongly up to temperatures in excess of 80 K. The positions of the light- and heavy-hole PLE transitions agrees well with the calculated energies, and the partial bleaching of the heavy-hole transition results from the buildup of the photogenerated hole density during the resonant excitation process.

For the sample doped at 2×10^{12} cm^{-2} the PL spectrum, (b), is much broadened with a high-energy Fermi tail. Such gross broadening is commonly observed for imperfect quantum-well structures in which strong hole

localization may occur.[28] Localization of the hole may allow **k** conservation for recombination transitions well away from the zone center. The spectra for the present sample are good examples of this strong localization limit, with transitions observed out to the Fermi wave vector $\mathbf{k}_F$, beyond which the spectrum is rapidly cut off by the decaying electron population. The Fermi tail of the PL spectrum and the tail of the PLE spectrum, with characteristic shape $[1-F(E)]$, match almost exactly, with no Stokes shift. We note that the PLE spectrum exhibited no resonance at the Fermi energy which might be ascribed to an FES. At higher energies the PLE spectrum exhibits an inflection which may be due to absorption into higher subbands. The PL Fermi cutoff, defined for this sample by the separation between E_F and the $n=1$ heavy-hole state, was calculated to be 1.619 eV; after correction for gap renormalization this reduces to 1.588 eV compared to the measured value of 1.59 eV.

The data for the highest doped well, (c), show a dramatic change in spectral shape, which results from recombination involving electrons from both the $n=1$ and 2 subbands. The extended luminescence plateau from the $n=1$ hole localized transitions remains, but now extends to higher energies. Recombinations involving the $n=2$ subbands is much more likely to be observed in this perturbed structure than in a conventional well because the perturbation results in only a 4-meV separation between the $n=1$ and 2 heavy-hole states, leading to strong hole population of the $n=2$ subband. The luminescence associated with the $n=2$ transitions produces a much less broadened peak near 1.61 eV. The calculated $n=2$ electron to $n=2$ heavy-hole separation, including 2D renormalization, is 1.607 eV, which is close to the measured peak energy. This energy is not, however, close to the calculated Fermi energy which is at 1.64 eV as indicated in Fig. 7. This location of the Fermi energy is confirmed by the PLE spectrum which exhibits no resonancelike features, but has a Fermi tail which fits reasonably well with the calculated value. The enhanced luminescence associated with the $n=2$ subbands may simply reflect the fact that zone-center transitions are mainly involved. The existence of a substantial Stokes shift for the $n=2$ related luminescence confirms that recombination does not occur from occupied states higher up the band. Certainly, the hole localization does not permit transitions from states out to $\mathbf{k}_F(n=2)$ which is much smaller than $\mathbf{k}_F(n=1)$. This implies that the hole localization is less significant than for the $n=1$ associated luminescence.

This may be understood on the assumption that a random potential associated with the δ plane is the origin of the localization. The localization effects would then be expected to be strongest in the center of the well, and to be symmetrical around the center. The overlap with particles of $n=1$ character is much stronger than for particles of $n=2$ character which have zero wave-function amplitude at the center of the well.[29] The perturbation arising from the δ sheet reduces the amplitude of the $n=1$ hole wave functions in the center of the well but only to approximately 50% of its maximum value, the maxima occurring symmetrically to either side of the δ cusp. Such a specifically located random potential is quite distinct from, say, width fluctuations, which influence all confined states regardless of the parity of the associated wave functions, and produce much larger broadening of the $n=2$ states.

V. CONCLUSIONS

Band-gap-related optical transitions associated with isolated δ doped layers are spatially indirect and hence very weak. This is a direct consequence of the potential barrier associated with the δ plane, which is repulsive to minority carriers. In this paper we have demonstrated that confinement of holes to the δ plane leads to strong luminescence; in particular we have shown that confinement in the quantum limit leads to truly spatially direct transitions. The quantum limit of confinement also leads to features in the optical spectra; new forms of low-dimensional structure result.

We have reported PL and PLE data from δ-plane superlattices and center-δ-doped quantum wells. For the superlattice structures, we have observed radiative transitions involving minibands or Δ bands, and confirmed the position of the Fermi level in these structures by PLE. We are able to account for the spectral information with self-consistent calculations of the subband structure. The radiative transitions involve only the electrons in the Δ bands and photogenerated holes trapped in the superlattice structure; such transitions have a much higher oscillator strength than is to be expected for spatially indirect transitions.

The mixed heterojunction-δ quantum-well systems exhibit subband structure, determined by the size confinement of both the δ sheet and the quantum well. Both electron and hole states are perturbed to an extent controlled by the δ concentration. Self-consistent solutions of the Poisson and (effective mass) Schrödinger equations predict large perturbations of subband energies; some of these features were confirmed from the PL and PLE data. Evidence for in-plane localization of photogenerated holes was also obtained from the spectroscopic data; the localization may result from the random potential associated with the δ plane.

ACKNOWLEDGMENTS

The authors gratefully acknowledge the support of the SERC for this work, which was carried out under the LDSD initiative. One of us (M.L.K.) wishes to thank the British Council and the government of the Peoples Republic of China for financial support. We wish to thank K. Ploog for helpful comments and J. Wagner for information prior to publication. We also wish to acknowledge the technical assistance of E. Lancake.

[1]R. C. Miller and D. A. Kleinman, J. Lumin. **30**, 520 (1985).
[2]S. Schmitt-Rink, C. Ell, and H. Haug, Phys. Rev. B **33**, 1183 (1986).
[3]E. F. Schubert, Y. Horikoschi, and K. Ploog, Phys. Rev. B **32**, 1085 (1989).
[4]B. Ulrich, C. Zhang, and K. von Klitzing, Appl. Phys. Lett. **54**, 1133 (1989).
[5]R. Cingolani, W. Stolz, and K. Ploog, Phys. Rev. B **40**, 2950 (1989).
[6]E. F. Schubert, A. Fischer, and K. Ploog, IEEE Trans. Electron. Dev. **ED-33**, 625 (1986).
[7]N. Schwarz, F. Müller, G. Tempel, F. Koch, and G. Weimann, Semicond. Sci. Technol. **4**, 571 (1989).
[8]J. A. Wagner, A. Ruiz, and K. Ploog, Phys. Rev. B **43**, 12 134 (1991).
[9]J. Wagner, A. Fischer, and K. Ploog, Phys. Rev. B **42**, 7280 (1990).
[10]J. A. Wagner, A. Fischer, and K. Ploog (private communication).
[11]P. Ruden and G. H. Dohler, Phys. Rev. B **27**, 3538 (1983).
[12]E. F. Schubert, B. Ullricht, T. D. Harris, and J. E. Cunningham, Phys. Rev. B **38**, 8305 (1988).
[13]A. C. Maciel, M. Tatham, J. F. Ryan, J. M. Worlock, R. E. Nahory, J. P. Harbison, and L. T. Florez, Surf. Sci. **228**, 251 (1990).
[14]H. Lee, W. J. Schaff, G. W. Wicks, L. F. Eastman, and A. R. Calawa, Institute of Physics Conference Series No. 74 (Institute of Physics and Physical Society, London, 1985), p. 321.
[15]E. F. Schubert, T. H. Chiu, J. E. Cunningham, B. Tell, and J. B. Stark, J. Electronic Mater. **17**, 527 (1988).
[16]A. Zrenner, F. Koch, R. L. Williams, R. A. Stradling, K. Ploog, and G. Weimann, Semicond. Sci. Technol. **3**, 1203 (1988).
[17]N. Schwarz, F. Müller, G. Tempel, F. Koch, and G. Weimann, Semicond. Sci. Technol. **4**, 571 (1989).
[18]J. S. Lee, Y. Awasa, and N. Miura, Semicond. Sci. Technol. **2**, 657 (1987).
[19]G. Livescu, D. A. B. Miller, D. S. Chelma, M. Ramaswamy, T. Y. Chang, N. Sauer, A. C. Gossard, and J. H. English, IEEE J. Quantum Electron **QE-24**, 1667 (1988).
[20]M. S. Skolnick, J. M. Rorison, K. J. Nash, D. J. Mowbray, P. R. Tapster, S. J. Bass, and A. D. Pitt, Phys. Rev. Lett. **58**, 2130 (1987).
[21]S. R. Andrews, A. S. Plaut, R. T. Harley, and T. M. Kerr, Phys. Rev. B **41**, 5040 (1990).
[22]R. B. Beall, J. B. Clegg, and J. J. Harris, Semicond. Sci. Technol. **3**, 612 (1988).
[23]E. F. Schubert, J. B. Stark, B. Ullrich, and J. E. Cunningham, Appl. Phys. Lett. **52**, 1508 (1988).
[24]A. Zrenner, F. Koch, and K. Ploog, Surf. Sci. **196**, 671 (1988).
[25]J. W. Orton *et al.*, Semicond. Sci. Technol. **2**, 597 (1987).
[26]S. Schmitt-Rink and C. Ell, J. Lumin. **30**, 585 (1985).
[27]H. Halt, K. Leo, R. Cingolani, and K. Ploog, Phys. Rev. B **40**, 12 017 (1989).
[28]M. A. Herman, D. Bimberg, and J. Christen, J. Appl. Phys. **70**, R1 (1991).
[29]W. Ted Masselink, Phys. Rev. Lett. **66**, 1513 (1991).